END

FILMED

DTIC

		1.0		4.5	2.8	2.5
				5.0		
				5.6	3.2	2.2
				6.3	3.6	
					4.0	2.0
		1.1				
						1.8
		1.25		1.4		1.6

MICROCOPY RESOLUTION TEST CHART
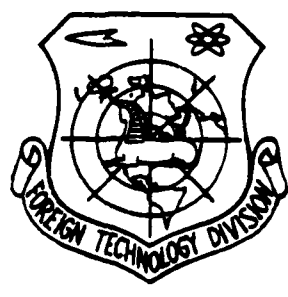NATIONAL BUREAU OF STANDARDS-1963-A

FOREIGN TECHNOLOGY DIVISION

ACTA AERONAUTICA ET ASTRONAUTICA SINICIA

(Selected Articles)

DTIC
ELECTE
JAN 2 4 1984
E

D

AD A137150

DTIC FILE COPY

84 01 24 062

EDITED TRANSLATION

Table of Contents

Accession For

NTIS GRA&I	☒
DTIC TAB	☐
Unannounced	☐
Justification	

By
Distribution/
Availability Codes

| Dist | Avail and/or Special |
| A-1 | |

GRAPHICS DISCLAIMER

All figures, graphics, tables, equations, etc. merged into this
translation were extracted from the best quality copy available.

ii

AN AZIMUTH RATE INERTIAL NAVIGATION SYSTEM

Ren Sicong (Northwestern Polytechnical University) and
Zhao Yongkang (Baocheng Instruments Factory)

Abstract

This paper proposes a new inertial navigation system combining the platform type and strap-down type inertial navigation systems. In this system, the azimuth rate platform without azimuth stabilized loop, azimuth coordinate resolver and synchronizer are used. The azimuth angles of the platform and vehicle are obtained by an integrator from azimuth rate signals measured by an azimuth gyroscope supported on a horizontal gimbal. This type of inertial navigation system is suitable for vehicles without large angle pitching maneuvers such as transports, aerodynamic and ballistic missiles etc. This paper discusses the operational principles of the azimuth rate platform, mechanization equations, distinguishing features of initial alignment, and the calibration and compensation for drifts of gyroscopes; at the same time, error propagation characteristics caused by various major error sources for navigation positioning, velocity and attitude are simulated on a computer. In the conclusion, we point out that the simplicity of the platform structure, small volume and weight, high reliability, and the possibility of calibration and compensation for drifts of the azimuth gyroscope are the outstanding advantages of this inertial navigation system. Furthermore, if we use a special optical system coordinated with known azimuth angles and latitudes of land marks, it is not only possible to realize fast alignment but also the calibration and compensation of horizontal gyroscopes.

I. Putting Forward the Problem and Brief Introduction of the Platform Structure

Even though there are presently many types of inertial navigation and guidance systems widely used in aeronautics, marine navigation as well as aerodynamic guided missiles, yet they can basically be summed up in the two large categories of the platform type and strap-down type.

The basic distinguishing features of the platform type system are that it uses a stabilized loop to separate the movements of the inertial device passing the gimbal and the vehicle thus causing them to be in an excellent operating environment and their dynamic ranges to be relatively small. It especially causes the influence of the gravitational acceleration to decrease to minimum when the semi-analytic type system is operating in a horizontal coordinate system. At the same time, the computed relationship is also relatively simple which proves the high accuracy of the system. However, the major drawbacks of the system are that the structure of the system is complex, manufacturing costs are very high, the volume and weight are relatively large and at the same time, the number of gimbals and slip rings are quite numerous so that the reliability is somewhat affected etc.

The inertial device of the strap-down system is directly strapped on the vehicle and thus its major advantages are its structure is simple, reliability good and the attitude information which does not require an electromechanical component for switching over has relatively high precision; however, the operating environment of the inertial device is adverse especially when the vehicle carries out sharp maneuvers as well as for their dynamic range which must be very wide and the extremely harsh requirements for the gyroscope. Furthermore, because the direction of the inertial device facing the gravitational field is constantly changing, the compensation technique for its errors and gravitational force is quite complex; requirements for the word length, speed and storage capacity of the computer are relatively high.

Therefore, we encounter very large difficulties in guaranteeing the operating precision of the strap-down system.

For a large number of vehicles, because of structural, mechanical and other specific reasons, when maneuvering, the angular rate difference of the roll and yaw movements is very far. For example, for common aircraft, when the roll angular rate can reach or exceed 360 degrees per second, the yaw angular rate is commonly only 2-3 degrees per second. The maximum cannot exceed 10 degrees per second. In this way, if we say we want to use a conventional inertial gyroscope to accurately measure the maximum angular rate of 10 degrees per second and not be able to have very great difficulties, it will be very difficult to use it to measure angular rates above 360 degrees per second. For just this reason, in order to fully bring into play the advantageous points of the platform and strap-down inertial navigation system, we propose a new azimuth rate inertial navigation system which can simplify the platform, lower the manufacturing costs and raise reliability. The platform which it uses eliminated the azimuth stabilized loop, azimuth coordinate resolver and azimuth synchronizer of the common three axis platform. The azimuth angles of the platform and vehicle are derived by an integrator from azimuth rate signals measured by an azimuth rate gyroscope supported on a horizontal gimbal.

When this type of system was first brought forth in 1978, it was called the "strap-down azimuth inertial navigation system" or the "semi-strap-down type inertial navigation system." Generally speaking, in order to simplify the platform, we can also have a "strap-down pitching system" and even an "azimuth and pitching strap-down system" which only has a roll stable axis. However, when we consider applying this system, it is most advantageous in a horizontal coordinate semi-analytical inertial navigation system with a not very large azimuth angle rate; it is basically the same as the "rotating azimuth",

3

"free azimuth", "drifting azimuth" and other systems. Further, when the platform has attitude errors, the azimuth gyroscope is also not completely "strapped" with the vehicle. In order to lose the meaning of "strapped-down" we therefore further changed the name to "azimuth rate" or "analytical azimuth" inertial navigation system.

The configuration of the azimuth rate platform is shown in Fig. 1. It can use two dual degrees of freedom gyroscopes or one single degree of freedom gyroscope. It can also be composed of one single degree of freedom angular rate and two single degree of freedom integrating gyroscopes.
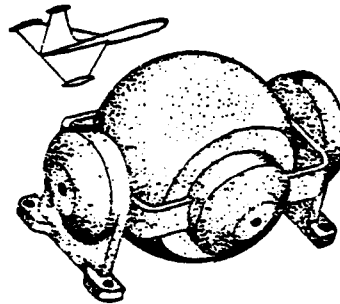

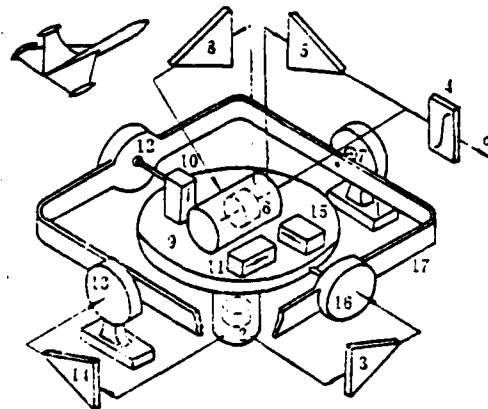Fig. 1   Configuration of the azimuth rate platform.

Fig. 2   Scheme of the azimuth rate platform.

Fig. 2 shows the principle of the azimuth rate platform

composed from two dual degrees of freedom gyroscopes. We can
see from the figure that the two dual degrees of freedom gyro-
scopes 2 and 6 and the three accelerometers 10, 11 and 15
installed on platform 9 form the inertial measuring component
supported by horizontal gimbal 17 and that the horizontal gimbal
is supported by the stand strapped together with vehicle 1. The
main axis of gyroscope 2 is in the plumb state during normal
operations and it uses corresponding amplifiers 3 and 14 as well
as stabilized electric machines 16 and 13 to realize stabiliza-
tion of the platform's pitch axis and roll axis; the main axis
of gyroscope 6 crosses with gyroscope 2 and uses amplifiers 5
and 8 to realize feedback self-locking and operates in a rate
condition. Because the feedback current of the passage surround-
ing the azimuth axis is the measurement of the azimuth angle
changing rate, integrator 4 can compute the azimuth angle.
Because the supporting axis line of the horizontal gimbal and
the longitudinal axis of the vehicle are parallel to eachother,
angular transucer 7 can put out roll attitude signals; cor-
respondingly, we obtain the pitch attitude signals from angular
transducer 12. It is very clear that this type of structure
simplifies the platform into a simple device which aside from the
azimuth gyroscope only has a horizontal gimbal similar to that of
the vertical gyroscope. However, when in pitch angles larger
than 60 degrees, the maneuvering movements of the vehicle pos-
sibly influence the normal operation of the platform. In order
to adapt to this type of situation, it is necessary to increase
the external rolling ring and corresponding stabilizing loop.

If the azimuth rate inertial navigation system is not used
for vehicles which make complete degree of freedom rolling and
pitching movements, the entire platform need not use the conduct-
ing slip ring but completely use the soft lead wire. This not
only simplifies the structure of the platform and makes main-
tenance convenient but even more important it can also raise
reliability.

5

Because the operating state of the azimuth rate gyroscope
is similar to that of the strap-down system, when compared with
the azimuth gyroscope of the common platform, its calibration
system errors and nonlinearity are possibly enlarged because
the dynamic range is relatively large; however, because the
vibration isolation of the horizontal gimbal and the platform are
basically in horizontal states, the gravitational effects are
relatively small and it is easy to guarantee the operating pre-
cision of the azimuth gyroscope. When we use the pulse rebal-
ance loop, this can also avoid the additional switching errors.

II. Mechanization Equations and Structural Block Diagram

We select the north, west and vector geographical coordinate
system NWV. As shown in Fig. 3, ideal platform system $X_T Y_T Z_T$
follows the vehcile rotating around vertical axis V and the
included angle of the X_T relative meridian N is platform azimuth
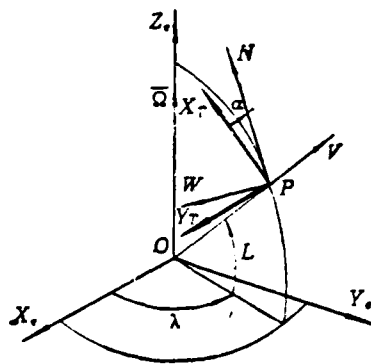angle α.

Fig. 3 Coordinate system.

Based on the specific power equation, we determine the
velocity of the platform relative to the earth from the following
differential equations:

6

$$\dot{V}_X = f_X - (2\Omega_Y + \omega_Y)V_Z + (2\Omega_{Zb} + \omega_{Zb})V_Y$$
$$\dot{V}_Y = f_Y - (2\Omega_{Zb} + \omega_{Zb})V_X + (2\Omega_X + \omega_X)V_Z \qquad (1)$$
$$\dot{V}_Z = f_Z - (2\Omega_X + \omega_X)V_Y + (2\Omega_Y + \omega_Y)V_X - g$$

In the equations, f_i is the specific power measured by the corresponding axis accelerometer; Ω_i is the earth's component; ω_i is the angular velocity component of the platform relative to the earth's rotation; g is the gravitational acceleration; and symbol b respresents the angular velocity of the platform driven by the vehicle.

In order to carry out navigation computations, we can use the relationship of the directional cosine matrix (C) formed from longitude λ, latitude L and azimuth angle α between the platform and earth system and its change rate, and the ω_i

$$[\dot{c}] = [C][\omega] \qquad (2)$$

In the formula

$$[C] = \begin{bmatrix} \sin\lambda\sin\alpha & \sin\lambda\cos\alpha & \cos L\cos\lambda \\ \begin{matrix}-\sin L\cos\lambda\cos\alpha \\ -\cos\lambda\sin\alpha\end{matrix} & \begin{matrix}\sin L\cos\lambda\sin\alpha \\ -\cos\lambda\cos\alpha\end{matrix} & \cos L\sin\lambda \\ \begin{matrix}-\sin L\sin\lambda\cos\alpha \\ \cos L\cos\alpha\end{matrix} & \begin{matrix}\sin L\sin\lambda\sin\alpha \\ -\cos L\sin\alpha\end{matrix} & \sin L \end{bmatrix} \qquad (3)$$

$$[\omega] = \begin{bmatrix} 0 & -\omega_{zb} & 0 \\ \omega_{zb} & 0 & -\omega_x \\ -\omega_Y & \omega_x & 0 \end{bmatrix} \qquad (4)$$

It is very clear that ω_X and ω_Y are derived based on V_Y and V_X and the earth's curvature is computed by computer and

7

bringing pressure on the gyroscope causes the platform to main-
tain a control quantity of a horizontal state. Thus, ω_{zb}
requires that Ω_{zb} be deleted from azimuth rate gyroscope
feedback control angular rate ω_{oZb}, that is

Further, when we consider the independent mixed attitude
system formed from the atmospheric pressure altitude information
and vertical accelerometer information, we can show the mechan-
ization relationship of the azimuth rate inertial navigation
system in the block diagram of Fig. 4.
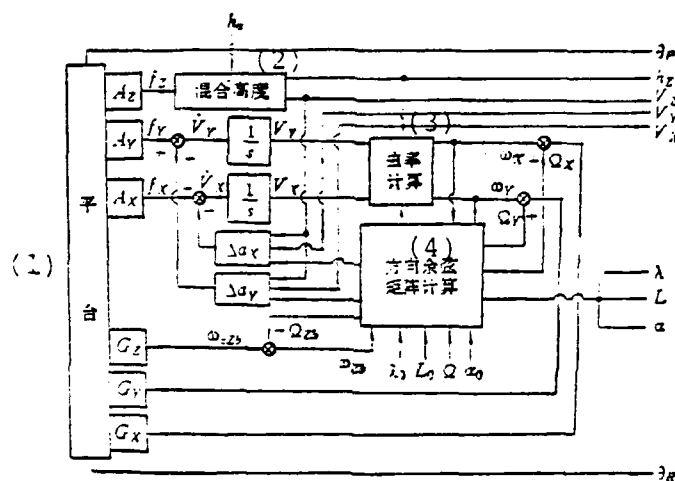
Fig. 4   Block diagram of the azimuth rate inertial navigation
          system.

          A_i and G_i are the accelerometer and gyroscope of the
          corresponding axis; h_a is the atmospheric pressure
          altitude information: θ_p and θ_R are the pitch and
          roll state information; λ_o and L_o are the initial
          longitude and latitude; Ω is the rotation angle rate
          of the earth.

III. Special Features of the Initial Alignment of the Azimuth
      Rate Platform

If we do not consider the structural errors, the azimuth of
the ideal platform system is also the parking position. For
just this reason, when we refer to the runway's middle line or

8

the special aircraft parking markers placed on the aircraft
parking area to determine the parking position of the aircraft,
we not only possibly realize fast speed alignment but can also
carry out calibration and compensation of the drifts of the
gyroscopes. In order to conveniently explain the problem, we
must first establish the attitude error equation. It is consid-
ered that when the attitude error angle is small in number we
can obtain

$$\bar{\varphi} = \bar{\omega}_P - C_T^r \bar{\omega}_T \qquad (6)$$

In the equation, $\bar{\varphi}$ is the attitude error angle vector;
$\bar{\omega}_T = \bar{\Omega} = [\Omega_X \ \Omega_Y \ \Omega_Z]^T$ is the angular rate vector of the ideal
platform system;

$$C_T^r = \begin{bmatrix} 1 & 0 & -\varphi_Y \\ 0 & 1 & \varphi_x \\ \varphi_Y & -\varphi_x & 1 \end{bmatrix}$$

is the attitude error matrix; $\bar{\omega}_P = \bar{\omega}_C + \bar{\omega}_{ZPP} + \bar{E}$ is the angular
rate vector of the platform system's rotation and
$\bar{\omega}_C = [\ \omega_{XC} \ \omega_{YC} \ 0]^T$ is the control added to the platform;
$\omega_{Zb}[0 \ 0 \ \Omega_{ZbP}]^T = [0 \ 0 \ \varphi_Y \Omega_X - \varphi_x \Omega_Y + \Omega_Z]^T$ is the angular
rate of the vehicle with platform rotation; $\bar{E} = [E_X E_Y 0]^T$ is the
shift angular rate of the platform.

By substituting the corresponding relationship into formula
(6) we obtain

$$\dot{\varphi}_x = \omega_{x\epsilon} - \Omega \cos L \cos \alpha + \varphi_Y \Omega \sin L + E_x$$
$$\dot{\varphi}_Y = \omega_{Y\epsilon} - \varphi_x \Omega \sin L + \Omega \cos L \sin \alpha + E_Y \qquad (7)$$
$$O = \Omega_{ZbP} - \varphi_Y \Omega \cos L \cos \alpha + \varphi_x \Omega \cos L \sin \alpha - \Omega \sin L$$

This formula shows that when the azimuth rate platform is in
initial alignment, the azimuth attitude errors do not produce
any changes. It also clearly reflects the basic special features
of this system's initial alignment. We can display formula (7)
as the block diagram shown in Fig. 5. In it, coefficients

9

K_1, K_2 and K_3 directly determine the dynamic characteristics of the leveling process. We should rationally make a selection based on the transient time and the basic requirements of anti-interference.

Under stable conditions, from formula (7) we obtain

$$\omega_{x_e}(\infty) = E_x - \Omega \cos L \cos \alpha$$

$$\omega_{y_e}(\infty) = E_y + \Omega \cos L \sin \alpha \tag{8}$$

From this, we can find the azimuth angle

$$\alpha_e = tg^{-1} \frac{-\omega_{y_e}(\infty)}{\omega_{x_e}(\infty)} = tg^{-1} \frac{\Omega \cos L \sin \alpha + E_y}{\Omega \cos L \cos \alpha - E_x} \tag{9}$$

It is very clear that the platform drift has direct influence on the calculation precision of the azimuth angle. Assuming $a_c = a + \Delta a$, and letting $\omega_{XC}(\infty) = \Omega \cos L \cos a$ and $\omega_{YC} = \Omega \cos L \sin a_c$, from formula (8) we can obtain

$$\Omega \cos L \sin \alpha \Delta \alpha = E_x$$

$$\Omega \cos L \cos \alpha \Delta \alpha = E_y \tag{10}$$

If we separately multiply this formula by sina and cosa and add them to eachother, we then find the calculation error of the azimuth angle is

$$\Delta \alpha = \frac{E_x \sin \alpha + E_y \cos \alpha}{\Omega \cos L} = \frac{E_w}{\Omega \cos L} \tag{11}$$

In the formula, $E_W = E_X \sin a + E_Y \cos a$ is the equivalent western drift of the platform. This conclusion is completely identical to other systems.

In order to calculate the compensation quantity of the drift, we can use the angular rate to calculate the earth's rotation and carry out compensation. Afterwards, we can find the

10

equivalent northern shift to be

$$E_{N_e} = \omega_{z_e}(\infty)\cos\alpha_e + \omega_{y_e}(\infty)\sin\alpha_e \approx E_x\cos\alpha_e + E_y\sin\alpha_e \qquad (12)$$

We then project it on a corresponding axis and obtain the compensation quantity of the shift

$$\hat{E}_x = E_{N_e}\cos\alpha_e \approx E_x\cos^2\alpha_e - E_y\sin\alpha_e\cos\alpha_e$$
$$\hat{E}_y = -E_{N_e}\sin\alpha_e \approx E_y\sin^2\alpha_e - E_x\cos\alpha_e\sin\alpha_e \qquad (13)$$

The errors after we use the above mentioned method to carry out compensation are

$$\delta E_x = \hat{E}_x - E_x = -(E_x\sin\alpha_e + E_y\cos\alpha_e)\sin\alpha_e$$

$$\delta E_y = \hat{E}_y - E_y = -(E_x\sin\alpha_e + E_y\cos\alpha_e)\cos\alpha_e \qquad (14)$$

The compensated errors are related to the equivalent western drift which cannot be measured.

After the leveling of the platform, $\Omega_{zb} = \Omega\sin L$ is a known quantity. When the gyroscope's precision coefficient K_G is known, based on the balance relationship $I(\infty) = K_G \Omega_{zb} - E_Z$ of the control current and azimuth angle rate, we can obtain the compensation quantity of the platform's azimuth drift.

$$\hat{E}_z = K_G\Omega\sin L - I(\infty) \qquad (15)$$

When we determine the accurate position of the runway or other land marks beforehand, by using a level viewing device, sighter or other special optical systems, we can determine the vehicle's longitudinal axis or the azimuth angle of the platform. In this way, we cannot only carry out fast speed alignment but the possibility also exists of calibrating the drift of the platform along the horizontal axis. In reality, when we assume the azimuth angle measured and introduced by computer is a_c, from

11

formula (8) we can then obtain

$$\overline{E}_x = \omega_{x_o}(\infty) + \Omega \cos L \cos \alpha - \Omega \cos L \cos \alpha_c$$

$$(16)$$

$$\overline{E}_Y = \omega_{Y_o}(\infty) - \Omega \cos L \sin \alpha + \Omega \cos L \sin \alpha_c$$

It is very clear that if there are no errors in the azimuth angle, the control value of the balanced state is equal to the drift of the platform. When the position error is Δa, we can obtain the compensation error of the drift quantity by using the relationship of $a_c = a + \Delta a$

$$\delta \overline{E}_x = \Omega \cos L \sin \alpha \Delta \alpha$$

$$(17)$$

$$\delta \overline{E}_Y = \Omega \cos L \cos \alpha \Delta \alpha$$

Naturally, when the precision of the moment device is very high and the structural errors of the platform are very small, the compensation quantity is equal to the drift of the gyroscope. It is very obvious that the precision of the platform's position and drift compensation are mainly determined by the measuring precision of the vehicle's longitudinal axis opposite the runway or land mark position as well as the measurement precision of the runway or the position of the land mark itself and the installation precision of the platform opposite the vehicle. It can be seen from formula (17) that when a=0, $\delta \overline{E}_X = 0$; when a=90°, $\delta \overline{E}_Y = 0$. This is completely the same as when carrying out calibration of common platforms. Further, the precision of the latitudes introduced by the computer is also related to the precision of compensation. For example, in overlooking the latitude errors, when L=a=45°, in order to cause $\delta \overline{E}_X$ and $\delta \overline{E}_Y$ to not be larger than 0.02°/hour, it is necessary to guarantee that azimuth error $\Delta a \leqslant 12'$. This data shows that only if the distance of the runway or land mark is not very short and the assembling

12

precision of the platform on the vehicle is also relatively high will this method have certain significance. Naturally, when we use optical methods and are able to cause the measurement precision of the azimuth angle to reach about 6', we can compensate the platform's drift close to 0.01°/hour.
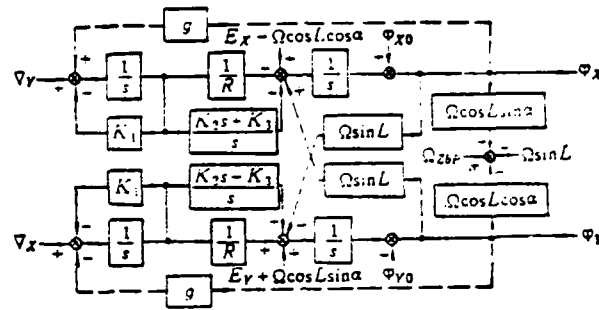

Fig. 5 Block diagram of initial alignment loops.

IV. Analogue Computations of Navigation Errors

In order to obtain an even more concrete understanding of the operating performance of the azimuth rate inertial navigation system, based on the fundamental relationship of formulas (1) and (2) as well as the corresponding error relationship, the calibration coefficient error of the gyroscope and accelerometer is $\Delta K_G = \Delta K_a = 1 \times 10^{-4}$; structural error $\delta_i = 20''$; gyroscope drift $\varepsilon_X = \varepsilon_Y = 0.01°/\text{hour}$ and $\varepsilon_Z = 0.02°/\text{hour}$; the accelerometer's zero position deviation $\nabla_X = \nabla_Y = 1 \times 10^{-4} g$; initial velocity $V_{XO} = V_{YO} = 0$; initial state error $\varphi_{XO} = \varphi_{YO} = 5 \times 10^{-4}$ radian; the theoretical position's initial value $L_O = 40°05'$, $\lambda_O = 116°36'$, $a_O = 45°00'$; and when the computation position's initial value $L_{cO} = 40°07'$, $\lambda_{cO} = 116°38'$, $a_{cO} = 45°03'$, we assume that the flight locus can be described by the following parameters:

13

$$a_x = \begin{cases} 3.3 & 0 < t \leqslant 30 \\ 2.0 & 30 < t \leqslant 60 \\ 1.0 & 60 < t \leqslant 200 \\ 0.0 & 200 < t \leqslant 4284 \\ -1.0 & 4284 < t \leqslant 4464 \\ -3.3 & 4464 < t \leqslant 4500 \end{cases} \quad \begin{matrix} (1) & (2) \\ (\text{米}/\text{秒}^2) & (\text{秒}) \end{matrix}$$

$$\omega_{zb} = \begin{cases} 0.0 & 0 < t \leqslant 60 \\ 1.5 & 60 < t \leqslant 240 \\ 0.0 & 240 < t \leqslant 4170 \\ -1.5 & 4170 < t \leqslant 4290 \\ 0.0 & 4290 < t \leqslant 4500 \end{cases} \quad \begin{matrix} (3) & (4) \\ (\text{度}/\text{秒}) & (\text{秒}) \end{matrix}$$

$$a_Y = \begin{cases} 0.0 & 0 < t \leqslant 60 \\ \omega_{zb}V_x & 60 < t \leqslant 240 \\ 0.0 & 240 < t \leqslant 4170 \\ \omega_{zb}V_x & 4170 < t \leqslant 4290 \\ 0.0 & 4290 < t \leqslant 4500 \end{cases} \quad \begin{matrix} (5) & (6) \\ (\text{米}/\text{秒}^2) & (\text{秒}) \end{matrix}$$

$$V_z = \begin{cases} 0.0 & 0 < t \leqslant 30 \\ V_x \text{tg}3.5^\circ & 30 < t \leqslant 60 \\ V_x \text{tg}1.0^\circ & 60 < t \leqslant 490 \\ 0.0 & 490 < t \leqslant 2970 \\ -V_x \text{tg}1^\circ & 2970 < t \leqslant 4248 \\ -V_x \text{tg}3^\circ & 4248 < t \leqslant 4464 \\ 0.0 & 4464 < t \leqslant 4500 \end{cases} \quad \begin{matrix} (7) & (8) \\ (\text{米}/\text{秒}) & (\text{秒}) \end{matrix}$$

Key: (1) Meters/second^2; (2) Seconds; (3) Degrees/
second; (4) Seconds; (5) Meters/second^2; (6) Seconds;
(7) Meters/second; (8) Seconds.

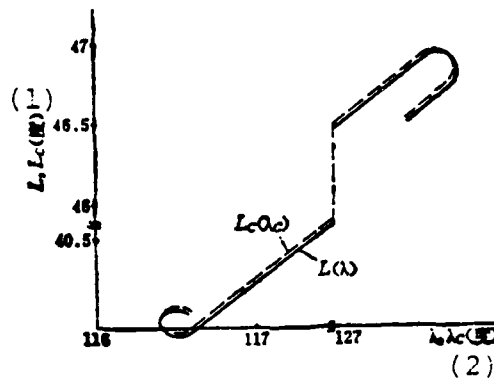The main computation results obtained are shown in Figs.
6-10.

Fig. 6 Flight course.
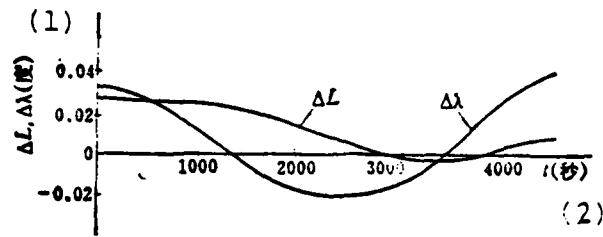Key: (1) Degrees; (2) Degrees.

14

Fig. 7   The time history of position errors.
Key: (1) Degrees; (2) Seconds.
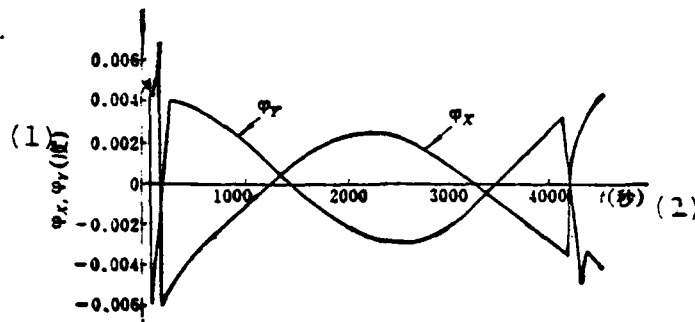

Fig. 8   The time history of attitude errors.
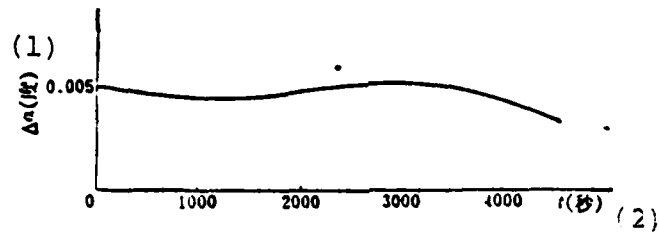Key: (1) Degrees; (2) Seconds.

Fig. 9   The time history of azimuth errors.
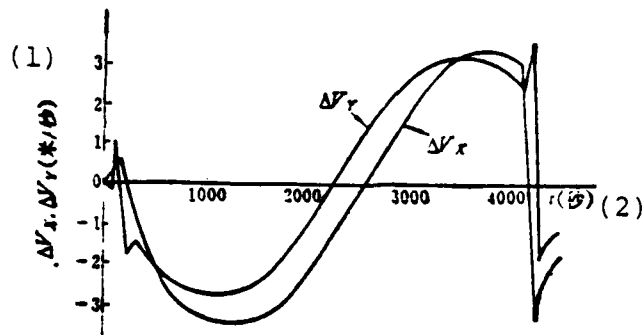Key: (1) Degrees; (2) Seconds.

15

Fig. 10   The time history of felocity errors.
Key: (1) Meters/second; (2) Seconds.

Fig. 6 shows the flight loci of aircraft taking off from an airfield runway, spiral climb, cruising, final returning and landing as well as other corresponding calculation values. It is very clear that the errors between the calculation and theoretical values change with the different courses and distances.

Fig. 7 gives the relational curve of the time history of position errors. We can see that basically they oscillate using the Schuler period; at the same time, the range of longitudinal error $\Delta\lambda$ is larger than latitudinal error ΔL. This is because when increasing with the latitude, the longitudinal value corresponding to the same type of distance error must be large.

Fig. 8 gives the relational curve of the time history of the platform's attitude errors. It can be clearly seen that because of the maneuvering flight of takeoff and landing, the attitude errors of the platform produce relatively intense changes with the different azimuth angles yet the maximum value is still within the allowable range. During the linear rate cruising stage, its law of oscillation coincides with the Schuler period.

The relationship of the time history of the azimuth angle

16

errors is shown in Fig. 9. It can be seen that the changes of
the azimuth angle errors are quite slow and their maximum value
does not exceed 0.06 degrees; when we consider that the initial
error is 3', the real change value is even smaller. When the
latitude is relatively high, the change quantity of the errors
is somewhat larger. This also tallies with the common laws.
To sum up, the output power here must be higher than when using
synchronizers and other electric machine transforming devices.
This also explains well the conclusion that the attitude errors
of the strap-down system must be smaller than when using the
output of the electric machine device for the platform system.

Fig. 10 gives the relational curve of the time history of
the velocity errors. We can see from the figure that during
takeoff and landing, because the velocity error is related to
the spiral angular rate, the changes are relatively intense.
However, calculating from the error changing curve of the
cruising stage, its period also coincides with the Schuler period.

V. Concluding Remarks

Based on the preceding discussion, we can see that the
azimuth rate inertial navigation system is relatively suitable
for vehicles with not very large changes in pitch and yaw atti-
tudes. It combines quite well the advantages of the platform
type and strap-down type inertial navigation systems and avoids
certain of their individual drawbacks. This type of platform
structure not only has few components, is simple in structure,
light in weight, has good reliability but moreover can provide
angular rate signals of the pilot's course damping channel.
Thus, it omits a course damping gyroscope and it can also give
course information with relatively high precision.

During each alignment, we can carry out calibration and com-
pensation of the azimuth drift of the platform. This is another

17

special advantage of this system. Moreover, if we use a known runway or land mark position and draw support from the level viewing device or other optical systems, we can also possibly realize fast speed alignment and the calibration and compensation of the horizontal drift. This is an area worthy of serious attention.

Because the azimuth angular rates of most vehicles are close to the angular rates of platform rotation in present rotating azimuth inertial navigation systems, there are no special conditions proposed for the requirements of the system's computer. Naturally, the software system is also close to the common semi-analytical inertial navigation system.

Finally, it should be pointed out that, relatively speaking, the drawbacks of the azimuth rate inertial navigation system are that it is not very suitable for fighters which perform stunt flying; because the platform itself does not have a degree of freedom around the azimuth axis, it is thus not convenient to carry out calibration and alignment of double positions but can only carry out single position alignment.

References

[1] J.C. Hong, The Strap-Down Type Navigation Platform, translated by Wang Kaiyuan, Science Press, 1979.

[2] Technical description of FERRENTI FIN1018C inertial NAV/ATTACK equipment, FERRENT LTD., 1979.

[3] Ren Sicong, Analysis of the Initial Alignment. Plan for a Vascillating Azimuth Intertial Navigation System, Inertial Navigation and Devices, No. 2, 1980.

OPTIMAL GUIDANCE LAWS FOR MISSILES WITH SECOND ORDER LINKS

Li Zhongying

Beijing Institute of Aeronautics and Astronautics

Abstract

This paper studies the optimal guidance laws for missiles with second order links aimed at targets. It uses the principle of the minimum to separately research: 1) when the target miss quantity is zero, the optimal guidance laws of the minimum control energy index; 2) when the final state is a zero control intercept curved surface, the optimal guidance laws of the minimum energy index. Finally, we obtained results similar to those for missiles with first order delay links.

Main Symbols

X_1	relative position vector of missile and target
X_2	relative velocity vector of missile and target
X_3	relative acceleration vector of missile and target
X_4	rate of change of relative acceleration vector
u	the missile control vector
$\bar{u}$	the missile's optimal control vector
ξ	the missile 's relative damping coefficient
ω	the missile body's intrinsic frequency
λ_i	conjugate state vector of state system
v, k	Lagrange multiplier, undetermined constant vector
t_o, t_f	separately the opening and final times
T	time to reach the zero control intercept curved surface
μ	time from reaching the zero control intercept curved surface to hitting the target
$\bar{\omega}$	angular velocity of line of sight between the missile and target
$\dot{\bar{\omega}}$	rate of change of angular velocity of line of sight
α, β	real numbers selected according to requirements

There has been a great deal of research [1,3,4,5] done both domestically and abroad on the optimal guidance laws for missiles. A great many beneficial results have been obtained which have had very good effects on realizing accurate guidance. However, the selected missile mathematical models have been too simple and generally all of them use particles with instantaneous response for processing. Reference [1] researched the optimal guidance laws of missiles with first order delay links. The results were composed of proportion guidance with a variable coefficient and correction items related to rate of change $\dot{\omega}$ of the line of sight angular velocity and acceleration a. However, the actual missile has non-instantaneous response particles and is not a first order delay link. The aim of this paper is to study the optimal guidance laws of missiles with second order links. Because its mathematical model is close to the real thing, the obtained results are beneficial for raising the guidance precision of the missile.

I. Formulation of the Problem

The relative motion dynamics model of the missile and target is

$$
\begin{cases}
\dot{x}_1 = x_2 & x_1(t_0) = x_{10} \\
\dot{x}_2 = x_3 & x_2(t_0) = x_{20} \\
\dot{x}_3 = x_4 & x_3(t_0) = x_{30} \\
\dot{x}_4 = -\omega^2 x_3 - 2\xi\omega x_4 + \omega^2 u & x_4(t_0) = 0
\end{cases}
\tag{1}
$$

The performance index is

$$
J(u) = \frac{1}{2} \int_{t_0}^{t_f} u^T \cdot u \, dt \quad (u^T \text{表示转置}) \tag{2}
$$

Key: (1) u^T indicates the transition position.

20

In the formula, $u \in R^3$ and t_f were given in advance. We assume the target group is

$$\begin{cases} g_1[x_1(t_f), x_2(t_f), x_3(t_f)] = 0 \\ g_2[x_1(t_f), x_2(t_f), x_3(t_f)] \leqslant 0 \end{cases} \qquad (3)$$

The present problem of finding the optimal control laws of dynamic system (1) so that the system is guided from the given initial state to final state (3) and moreover cause perform- ance index (2) to adopt a very small value.

Below, we will seek the optimal guidance laws for two dif- ferent types of target groups.

II. The Zero Miss Minimum Energy Guidance Law

The target group is
$$x_1(t_f) = 0$$

The other parameters of the terminal are free.

Based on the principle of the maximum [2], the problem's Hamiltonian function H is:

$$H = \frac{1}{2} u^T \cdot u + \lambda_1^T \cdot x_2 + \lambda_2^T \cdot x_3 + \lambda_3^T \cdot x_4 + \lambda_4^T (-\omega^2 x_3 - 2\xi\omega x_4 + \omega^2 u) \qquad (4)$$

In the formula, λ_1, λ_2, λ_3 and λ_4 are the conjugate state vectors of the dynamic system (1).

$$\begin{cases} \lambda_1(t) = 0 \\ \lambda_2(t) = -\lambda_1(t) \\ \lambda_3(t) = -\lambda_2(t) - \omega^2\lambda_4(t) \\ \lambda_4(t) = -\lambda_3(t) - 2\xi\omega\lambda_4(t) \end{cases} \qquad (5)$$

Their cross section conditions are

$$\begin{cases} \lambda_1(t_f) = v \\ \lambda_2(t_f) = 0 \\ \lambda_3(t_f) = 0 \\ \lambda_4(t_f) = 0 \end{cases} \qquad (6)$$

Based on the principle of the minimum, the optimal control laws and corresponding conjugate state parameters should cause the H function to take the minimum value and from

$$\frac{\partial H}{\partial u} = 0$$

we obtain

$$\bar{u}(t) = -\omega^2 \lambda_4(t) \qquad (7)$$

We can see from formula (7) that to determine the optimal control laws, we must determine conjugate state vector $\lambda_4(t)$.

From the first two equations in equation group (5) and the corresponding boundary conditions, we can solve

$$\lambda_1(t) = v$$
$$\lambda_2(t) = v(t_f - t)$$

Therefore, we have

$$\lambda_3(t) = -v(t_f - t) + \omega^2 \lambda_4(t) \qquad (8)$$

We then seek a derivative of the fourth equation of equation group (5) and obtain

$$\ddot{\lambda}_4(t) = -\lambda_3(t) + 2\xi\omega\dot{\lambda}_4(t)$$

Then we substitute in formula (8) we obtain

$$\ddot{\lambda}_4(t) - 2\xi\omega\dot{\lambda}_4(t) + \omega^2\lambda_4(t) = v(t_f - t) \qquad (9)$$

22

We can know from formula (7) that to find the optimal control laws it is only necessary to solve $\lambda_4(t)$. In equation (9), we let

$$\tau = t_f - t$$

and therefore equation (9) becomes

$$\ddot{\lambda}_4(\tau) + 2\xi\omega\dot{\lambda}_4(\tau) + \omega^2\lambda_4(\tau) = v\tau \tag{9'}$$

When $\tau = 0$, $t = t_f$ has $\lambda_4(0) = 0$ and moreover we suppose $\dot{\lambda}_4(0) = 0$. Formula (9)' is a second order non-homogeneous linear differential equation with a constant coefficient. We can find its solution by using the Laplace transformation:

$$\lambda_4(\tau) = \frac{v\tau}{\omega^2} - \frac{2\xi v}{\omega^3} + \frac{ve^{-\xi\omega\tau}}{\omega^3}\left[2\xi\cos\Omega\tau + \frac{2\xi^2 - 1}{(1-\xi^2)^{1/2}}\sin\Omega\tau\right] \tag{10}$$

In the formula,

$$\Omega = \omega(1 - \xi^2)^{1/2}$$

By substituting formula (10) into formula (7), we can obtain the optimal control law:

$$\bar{u}(t) = -v\left\{(t_f - t) - \frac{2\xi}{\omega} + \frac{1}{\omega}e^{-\xi\omega(t_f - t)}\left[2\xi\cos\Omega(t_f - t)\right.\right.$$
$$\left.\left. + \frac{2\xi^2 - 1}{(1-\xi^2)^{1/2}}\sin\Omega(t_f - t)\right]\right\} \tag{11}$$

For the final determination of the optimal control law, we must determine constant vector v and for this reason we must substitute formula (11) into the system's state equation group (1) to solve the state parameters.

From the third equation in equation group (1) we have

$$\ddot{x}_3(t) = \dot{x}_4(t)$$

23

When we substitute the fourth equation in equation group (1) into the above equation, we obtain

$$\ddot{x}_3(t) = -\omega^2 x_3(t) - 2\xi\omega x_4(t) + \omega^2 \bar{u}(t)$$

We then substitute the third equation in equation group (1) into the above equation and obtain

$$\ddot{x}_3(t) + 2\xi\omega\dot{x}_3(t) + \omega^2 x_3(t) = \omega^2 \bar{u}(t)$$

We substitute formula (11) into this equation and obtain

$$\ddot{x}_3 + 2\xi\omega\dot{x}_3 + \omega^2 x_3 = -v\omega^2\left\{(t_f - t) - \frac{2\xi}{\omega} + \frac{1}{\omega}e^{-\xi\omega(t_f-t)}\left[2\xi\cos\Omega(t_f - t)\right.\right.$$
$$\left.\left. + \frac{2\xi^2 - 1}{(1-\xi^2)^{1/2}}\sin\Omega(t_f - t)\right]\right\} \tag{12}$$

This is also a non-homogeneous linear differential equation with a second order constant coefficient which can still be solved by the Laplace transformation. Finally, we obtain

$$x_3(t) = -v\left\{(t_f - t) - \left[t_f^2 + \frac{(\xi\omega t_f + 1)^2}{\Omega^2}\right]^{1/2}e^{-\xi\omega t}\sin(\Omega t + \psi_1)\right.$$
$$-\frac{1}{4\omega(1-\xi^2)^{1/2}}e^{-\xi\omega(t_f-t)}\sin[\Omega(t_f - t) + \psi_0]$$
$$-(a^2+b^2)^{1/2}e^{-\xi\omega(t_f-t)}\cos(\Omega t + \psi_3) - \frac{1}{4\omega(1-\xi^2)^{1/2}}e^{-\xi\omega(t_f-t)}\sin[\Omega(t_f - t) + \psi_0]$$
$$\left. + \frac{\Omega}{4\xi\omega^2(1-\xi^2)^{1/2}}e^{-\xi\omega(t_f-t)}\cos[\Omega(t_f - t) + \psi_0]\right\} + x_{30}\frac{1}{1-\xi^2}e^{-\xi\omega t}\cos(\Omega t + \psi_2) \tag{13}$$

In the formula

24

$$\psi_0 = \mathrm{tg}^{-1}\left[\frac{2\xi(1-\xi^2)^{1/2}}{2\xi^2-1}\right]$$

$$\psi_1 = \mathrm{tg}^{-1}\left[\frac{\Omega t_f}{\xi\omega t_f + 1}\right]$$

$$\psi_2 = \mathrm{tg}^{-1}\left[\frac{\xi\omega}{\Omega}\right]$$

$$\psi_3 = \mathrm{tg}^{-1}\left[\frac{1+\xi^2}{1-\xi^2}\mathrm{tg}(\Omega t_f + \psi_0)\right]$$

$$a = \frac{\Omega}{4\xi\omega^2(1-\xi^2)^{1/2}}\cos(\Omega t_f + \psi_0)$$

$$b = \frac{(1+\xi^2)\Omega}{4\xi\omega^2(1-\xi^2)^{1/2}}\sin(\Omega t_f + \psi_3)$$

They are all the missile body's known characteristic parameters ξ and ω as well as the function terminal time t_f. When t_f is given, it is an unchanging constant.

Based on the first equation in equation group (1) and its initial conditions, by substituting in formula (13) and integrating we can obtain

$$
\begin{aligned}
x_2(t) = & x_{20} + \frac{x_{30}}{\omega(1-\xi^2)}\left[e^{-\xi\omega t_0}\cos(\Omega t_0 + \psi_0 + \psi_2) - e^{-\xi\omega t}\cos(\Omega t + \psi_0 + \psi_2)\right] \\
& - v\left\{\left(t_f t - \frac{t^2}{2}\right) + \left[t_f^2 + \frac{(\xi\omega t_f + 1)^2}{\Omega^2}\right]^{1/2}\frac{e^{-\xi\omega t}}{\omega}\sin(\Omega t + \psi_1 + \psi_2)\right.\\
& + \frac{(a^2+b^2)^{1/2}}{\omega}e^{-\xi\omega(t_f + t)}\cos(\Omega t + \psi_3 + \psi_2) + \frac{e^{-\xi\omega(t_f - t)}}{4\omega^2(1-\xi^2)^{1/2}}\sin[\Omega(t_f - t) + \psi_0 - \psi_2] \\
& - \frac{e^{-\xi\omega(t_f - t)}}{4\omega^2(1-\xi^2)^{1/2}}\sin[\Omega(t_f - t) + \psi_0 + \psi_2] + \frac{\Omega e^{-\xi\omega(t_f - t)}}{4\xi\omega^3(1-\xi^2)^{1/2}}\cos[\Omega(t_f - t) \\
& \left. + \psi_0 + \psi_2] - \left(t_f t_0 - \frac{t_0^2}{2}\right) + C_1(t_f, t_0, \xi, \omega)\right\}
\end{aligned}
\tag{14}
$$

In the formula

$$C_1(t_f, t_0, \xi, \omega) = -\left[t_f^2 + \frac{(\xi \omega t_f + 1)^2}{\Omega^2} \right]^{1/2} \frac{e^{-\xi \omega t_0}}{\omega} \sin(\Omega t_0 + \psi_1 + \psi_4)$$

$$- \frac{(a^2 + b^2)^{1/2}}{\omega} e^{-\xi \omega (t_f + t_0)} \cos(\Omega t_0 + \psi_3 + \psi_4) - \frac{1}{4\omega^2 (1 - \xi^2)^{1/2}} \{ e^{-\xi \omega (t_f + t_0)} \sin[\Omega(t_f - t_0)]$$

$$+ \psi_0 - \psi_4] - e^{-\xi \omega (t_f - t_0)} \sin[\Omega(t_f - t_0) + \psi_0 + \psi_4] \} - \frac{\Omega e^{-\xi \omega (t_f - t_0)}}{4\xi \omega^3 (1 - \xi^2)^{1/2}} \cos[\Omega(t_f - t_0)$$

$$+ \psi_0 + \psi_4]$$

$$\psi_4 = \mathrm{tg}^{-1}\left[\frac{\Omega}{\xi \omega} \right]$$

Based on the first equation in equation group (1) and its initial conditions, we substitute in formula (14), integrate once and obtain

$$x_1(t) = x_{10} + x_{20}(t - t_0) + \frac{x_{30}}{\omega(1 - \xi^2)}\left[e^{-\xi \omega t_0}(t - t_0)\cos(\Omega t_0 + \psi_0 + \psi_4) \right.$$

$$- \frac{e^{-\xi \omega t_0}}{\omega}\cos(\Omega t_0 + \psi_0 + 2\psi_4) + \frac{e^{-\xi \omega t}}{\omega}\cos(\Omega t + \psi_0 + 2\psi_4) \left. \right]$$

$$\doteq v \left\{ \left(t_f \frac{t^2}{2} - \frac{t^3}{6} \right) - \left[t_f^2 + \frac{(\xi \omega t_f + 1)^2}{\Omega^2} \right]^{1/2} \frac{e^{-\xi \omega t}}{\omega}\sin(\Omega t + \psi_1 + 2\psi_4) \right.$$

$$- \frac{(a^2 + b^2)^{1/2}}{\omega^2} e^{-\xi \omega (t_f + t)}\cos(\Omega t + \psi_3 + \psi_4) + \frac{e^{-\xi \omega (t_f + t)}}{4\omega^3 (1 - \xi^2)^{1/2}}\sin[\Omega(t_f - t) + \psi_0 - 2\psi_4]$$

$$- \frac{e^{-\xi \omega (t_f - t)}}{4\omega^3 (1 - \xi^2)^{1/2}}\sin[\Omega(t_f - t) + \psi_0 + 2\psi_4] + \frac{\Omega e^{-\xi \omega (t_f - t)}}{4\xi \omega^4 (1 - \xi^2)^{1/2}}\cos[\Omega(t_f - t) + \psi_0 + 2\psi_4]$$

$$- \left(t_f t_0 - \frac{t_0^2}{2} \right) t + C_1(t_f, t_0, \xi, \omega) t + \left(\frac{t_f t_0^2}{2} - \frac{t_0^3}{3} \right) + C_0(t_f, t_0, \xi, \omega) \left. \right\} \qquad (15)$$

In the formula

$$C_0(t_f, t_0, \xi, \omega) = -C_1(t_f, t_0, \xi, \omega) t_0 + \left[t_f^2 + \frac{(\xi \omega t_f + 1)^2}{\Omega^2} \right]^{1/2} \frac{e^{-\xi \omega t_0}}{\omega^2}$$

$$\times \sin[\Omega t_0 + \psi_1 + 2\psi_4] + \frac{(a^2 + b^2)^{1/2}}{\omega^2} e^{-\xi \omega (t_f + t_0)}\cos(\Omega t_0 + \psi_3 + \psi_4)$$

$$- \frac{e^{-\xi \omega (t_f + t_0)}}{4\omega^3 (1 - \xi^2)^{1/2}}\sin[\Omega(t_f - t_0) + \psi_0 - 2\psi_4] + \frac{e^{-\xi \omega (t_f - t_0)}}{4\omega^3 (1 - \xi^2)^{1/2}}\sin[\Omega(t_f - t_0) + \psi_0 + 2\psi_4]$$

$$- \frac{\Omega e^{-\xi \omega (t_f - t_0)}}{4\xi \omega^4 (1 - \xi^2)^{1/2}}\cos[\Omega(t_f - t_0) + \psi_0 + 2\psi_4]$$

From $x_1(t_f)=0$ we can determine constant vector v.

$$
\begin{aligned}
v = \Big\{ &x_{10} + x_{20}(t_f - t_0) + \frac{x_{30}}{\omega(1-\xi^2)}\Big[e^{-\xi\omega t_0}(t_f - t_0)\cos(\Omega t_0 + \psi_0 + \psi_4) \\
&- \frac{e^{-\xi\omega t_0}}{\omega}\cos(\Omega t_0 + \psi_0 + 2\psi_4) + \frac{e^{-\xi\omega t_f}}{\omega}\cos(\Omega t_f + \psi_0 + 2\psi_4)\Big] \times \Big\{\frac{(t_f - t_0)^3}{3} \\
&- \Big[t_f^2 + \frac{(\xi\omega t_f + 1)^2}{\Omega^2}\Big]^{1/2} \frac{e^{-\xi\omega t_f}}{\omega^2}\sin(\Omega t_f + \psi_1 + 2\psi_4) - \frac{(a^2 + b^2)^{1/2}}{\omega^2}e^{-2\xi\omega t_f}\cos(\Omega t_f + \psi_3 + \psi_4) \\
&+ \frac{e^{-2\xi\omega t_f}}{4\omega^3(1-\xi^2)^{1/2}}\sin(\psi_0 - 2\psi_4) - \frac{1}{4\omega^3(1-\xi^2)^{1/2}}\sin(\psi_0 + 2\psi_4) + \frac{\Omega}{4\xi\omega^4(1-\xi^2)^{1/2}} \\
&\times \cos(\psi_0 + 2\psi_4) + C_1(t_f, t_0, \xi, \omega)t_f + C_0(t_f, t_0, \xi, \omega)\Big\}^{-1}
\end{aligned}
\tag{16}
$$

We substitute the v value into formula (11) and obtain

$$
\begin{aligned}
\bar{u}(t) = -\Big\{ &x_{10} + x_{20}(t_f - t_0) + \frac{x_{30}}{\omega(1-\xi^2)}\Big[e^{-\xi\omega t_0}(t_f - t_0)\cos(\Omega t_0 + \psi_0 + \psi_4) \\
&- \frac{e^{-\xi\omega t_0}}{\omega}\cos(\Omega t_0 + \psi_0 + 2\psi_4) + \frac{e^{-\xi\omega t_f}}{\omega}\cos(\Omega t_f + \psi_0 + 2\psi_4)\Big] \times \Big\{(t_f - t) \\
&- \frac{2\xi}{\omega} + \frac{e^{-\xi\omega(t_f - t)}}{\omega}\Big[2\xi\cos\Omega(t_f - t) + \frac{2\xi^2 - 1}{(1-\xi^2)^{1/2}}\sin\Omega(t_f - t)\Big]\Big\} \times \Big\{\frac{(t_f - t_0)^3}{3} \\
&- \Big[t_f^2 + \frac{(\xi\omega t_f + 1)^2}{\Omega^2}\Big]^{1/2} \frac{e^{-\xi\omega t_f}}{\omega^2}\sin(\Omega t_f + \psi_1 + 2\psi_4) - \frac{(a^2 + b^2)^{1/2}}{\omega^2}e^{-2\xi\omega t_f}\cos(\Omega t_f + \psi_3 + \psi_4) \\
&+ \frac{e^{-2\xi\omega t_f}}{4\omega^3(1-\xi^2)^{1/2}}\sin(\psi_0 - 2\psi_4) - \frac{1}{4\omega^3(1-\xi^2)^{1/2}}\sin(\psi_0 + 2\psi_4) + \frac{\Omega}{4\xi\omega^4(1-\xi^2)^{1/2}} \\
&\times \cos(\psi_0 + 2\psi_4) + C_1(t_f, t_0, \xi, \omega)t_f + C_0(t_f, t_0, \xi, \omega)\Big\}^{-1}
\end{aligned}
\tag{17}
$$

Letting

$$
\begin{aligned}
F(t_f, t_0, \xi, \omega) = &-\Big[t_f^2 + \frac{(\xi\omega t_f + 1)^2}{\omega^2}\Big]^{1/2} \frac{e^{-\xi\omega t_f}}{\omega^2}\sin(\Omega t_f + \psi_1 + 2\psi_4) - \frac{(a^2 + b^2)^{1/2}}{\omega^2} \\
&\times e^{-2\xi\omega t_f}\cos(\Omega t_f + \psi_3 + \psi_4) + \frac{e^{-2\xi\omega t_f}}{4\omega^3(1-\xi^2)^{1/2}}\sin(\psi_0 - 2\psi_4) - \frac{1}{4\omega^3(1-\xi^2)^{1/2}} \\
&\times \sin(\psi_0 + 2\psi_4) + \frac{\Omega}{4\xi\omega^4(1-\xi^2)^{1/2}}\cos(\psi_0 + 2\psi_4) + C_1(t_f, t_0, \xi, \omega)t_f \\
&+ C_0(t_f, t_0, \xi, \omega)
\end{aligned}
$$

When t_f is given, $F(t_f, t_0, \xi, \omega)$ is a constant quantity determined by the missile body's parameters ξ, ω and time t_0. In this way, formula (17) can be simplified into

27

$$\bar{u}(t) = -\left\{ x_{10} + x_{20}(t_f - t_0) + \frac{x_{30}}{\omega(1-\xi^2)}\left[e^{-\xi\omega t_0}(t_f - t_0)\cos(\Omega t_0 + \psi_0 + \psi_4) \right.\right.$$

$$\left. - \frac{e^{-\xi\omega t_0}}{\omega}\cos(\Omega t_0 + \psi_0 + 2\psi_4) + \frac{e^{-\xi\omega t_f}}{\omega}\cos(\Omega t_f + \psi_0 + 2\psi_4) \right] \times \left\{ (t_f - t) \right.$$

$$\left. - \frac{2\xi}{\omega} + \frac{e^{-\xi\omega(t_f - t)}}{\omega}\left[2\xi\cos\Omega(t_f - t) + \frac{2\xi^2 - 1}{(1-\xi^2)^{1/2}}\sin\Omega(t_f - t) \right] \right\}$$

$$\times \left\{ \frac{(t_f - t)^3}{3} + F(t_f, t_0, \xi, \omega) \right\}^{-1} \tag{18}$$

When $t = t_0$, the optimal guidance law is

$$\bar{u}(t_0) = -\left\{ x_{10} + x_{20}(t_f - t_0) + \frac{x_{30}}{\omega(1-\xi^2)}\left[e^{-\xi\omega t_0}(t_f - t_0)\cos(\Omega t_0 + \psi_0 + \psi_4) \right.\right.$$

$$\left. - \frac{e^{-\xi\omega t_0}}{\omega}\cos(\Omega t_0 + \psi_0 + 2\psi_4) + \frac{e^{-\xi\omega t_f}}{\omega}\cos(\Omega t_f + \psi_0 + 2\psi_4) \right\} \times \left\{ (t_f - t_0) \right.$$

$$\left. - \frac{2\xi}{\omega} + \frac{e^{-\xi\omega(t_f - t_0)}}{\omega}\left[2\xi\cos\Omega(t_f - t_0) + \frac{2\xi^2 - 1}{(1-\xi^2)^{1/2}}\sin\Omega(t_f - t_0) \right] \right\} \times \left\{ \frac{(t_f - t_0)^3}{3} \right.$$

$$\left. + F(t_f, t_0, \xi, \omega) \right\}^{-1} \tag{19}$$

We let

$$K(t_f, t_0, \xi, \omega) = \left\{ (t_f - t_0) - \frac{2\xi}{\omega} + \frac{e^{-\xi\omega(t_f - t_0)}}{\omega(1-\xi^2)}\sin[\Omega(t_f - t_0) + \psi_0] \right\}$$

$$\times \left\{ \frac{(t_f - t_0)^3}{3} + F(t_f, t_0, \xi, \omega) \right\}^{-1}$$

$$L(t_f, t_0, \xi, \omega) = \frac{1}{\omega(1-\xi^2)}\left[e^{-\xi\omega t_0}(t_f - t_0)\cos(\Omega t_0 + \psi_0 + \psi_4) - \frac{e^{-\xi\omega t_0}}{\omega} \right.$$

$$\left. \times \cos(\Omega t_0 + \psi_0 + 2\psi_4) + \frac{e^{-\xi\omega t_f}}{\omega}\cos(\Omega t_f + \psi_0 + 2\psi_4) \right] \times \left\{ (t_f - t_0) - \frac{2\xi}{\omega} \right.$$

$$\left. + \frac{e^{-\xi\omega(t_f - t_0)}}{\omega(1-\xi^2)}\sin[\Omega(t_f - t_0) + \psi_0] \right\} \times \left\{ \frac{(t_f - t_0)^3}{3} + F(t_f, t_0, \xi, \omega) \right\}^{-1}$$

In this way, formula (19) is simplified into

$$\bar{u}(t_0) = -K(t_f, t_0, \xi, \omega)[x_{10} + x_{20}(t_f - t_0)] - L(t_f, t_0, \xi, \omega)x_{30} \tag{20}$$

The guidance law shown by formula (20) can use the appropriate selection time $t_f - t_0$ which can change it into proportional guidance with a variable coefficient (in proportion to the line of vision angular velocity) and the guidance law [1] composed of

28

correction items with one item related to the acceleration and line of vision angular acceleration.

When $\mathcal{Q} \rightarrow \infty$, the dynamic response process of the missile is lost, that is, the response of the system is without oscillation as well as without delay. At this time, $F(t_f, t_o, \xi, \mathcal{Q}) \doteq 0$.

$$K(t_f, t_o, \xi, \omega) = \frac{3}{(t_f - t_o)^2}$$
$$L(t_f, t_o, \xi, \omega) = 0$$

Therefore

$$\bar{u}(t_o) = -\frac{3[x_{10} + x_{20}(t_f - t_o)]}{(t_f - t_o)^2} \tag{21}$$

This is the optimal guidance law of the instantaneous response particles. After selecting the different t_f-t_o values, we can obtain the proportional guidance law of the various different systems [3].

III. Guidance Laws of the Target Group as a Zero Control Intercept Curved Surface

When dynamic system (1) is guided towards zero control intercept curved surface L, its target groups is [1,2]:

$$\begin{cases} x_1(T) + \mu x_2(T) = 0, & \mu \geq 0 \\ x_2(T) = 0 \end{cases} \tag{22}$$

It is assumed that the introduced time T of the zero control intercept curved surface L is already selected; time μ from entering the zero control intercept curved surface to hitting the target is undetermined.

The main reason why $x_3(T) = 0$ is necessary is because it is

required that we cause the system to be able to be maintained within this curved surface after bringing the system into the zero control intercept curved surface.

The performance index is still formula (2) and at this time Hamiltonian function H of the system does not change. Thus, the conjugate state set of equations of dynamic system (1) is still described by formula (5). However, the cross section conditions change to

$$
\begin{cases}
\lambda_1(T) = v \\
\lambda_2(T) = v\mu \\
\lambda_3(T) = k \\
\lambda_4(T) = 0
\end{cases} \tag{23}
$$

In the formula, v and k are Lagrange multipliers which are undetermined constant vectors. Based on these boundary conditions solving conjugate state set of equations (5), we obtain:

$$
\begin{aligned}
\lambda_1(t) &= v \\
\lambda_2(t) &= v(T + \mu - t) \\
\lambda_3(t) &= -v(T + \mu - t) + \omega^2 \lambda_4(t) \\
\ddot{\lambda}_4(t) &= 2\xi\omega\dot{\lambda}_4(t) - \omega^2 \lambda_4(t) + v(T + \mu - t)
\end{aligned}
$$

Based on the results in Section II, we obtain

$$
\lambda_4(t) = \frac{v}{\omega^2}\left\{(T + \mu - t) - \frac{2\xi}{\omega} + \frac{1}{\omega}e^{-\xi\omega(T+\mu-t)}\left[2\xi\cos\Omega(T + \mu - t) + \frac{2\xi^2 - 1}{(1 - \xi^2)^{1/2}}\sin\Omega(T + \mu - t)\right]\right\} \tag{24}
$$

When we substitute $\lambda_4(t)$ into formula (7), we obtain the optimal guidance law

$$
\bar{u}(t) = -v\left\{(T + \mu - t) - \frac{2\xi}{\omega} + \frac{1}{\omega}e^{-\xi\omega(T+\mu-t)}\left[2\xi\cos\Omega(T + \mu - t) + \frac{2\xi^2 - 1}{(1 - \xi^2)^{1/2}}\sin\Omega(T + \mu - t)\right]\right\} \tag{25}
$$

30

When we substitute formula (25) into dynamic system (1), just as in Section II we can solve $x_3(t)$, $x_2(t)$ and $x_1(t)$.

$$x_3(t) = -v\left\{(T+\mu-t) - \left[(T+\mu)^2 + \frac{(\xi\omega(T+\mu)+1)^2}{\Omega^2}\right]^{1/2} e^{-\xi\omega t}\sin(\Omega t+\psi_1)\right.$$

$$-\frac{e^{-\xi\omega(T+\mu+t)}}{4\omega(1-\xi^2)^{1/2}}\sin[\Omega(T+\mu-t)+\psi_0] - (a^2+b^2)^{1/2}e^{-\xi\omega(T+\mu+t)}$$

$$\times\cos(\Omega t+\psi_3) - \frac{e^{-\xi\omega(T+\mu-t)}}{4\omega(1-\xi^2)^{1/2}}\sin[\Omega(T+\mu-t)+\psi_0]$$

$$\left.+\frac{\Omega e^{-\xi\omega(T+\mu-t)}}{4\xi\omega^2(1-\xi^2)^{1/2}}\cos[\Omega(T+\mu-t)+\psi_0]\right\} + \frac{x_{30}}{1-\xi^2}e^{-\xi\omega t}\cos(\Omega t+\psi_2) \qquad (26)$$

$$x_2(t) = x_{20} + \frac{x_{30}}{\omega(1-\xi^2)}\left[e^{-\xi\omega t_0}\cos(\Omega t_0+\psi_0+\psi_4) - e^{-\xi\omega t}\cos(\Omega t+\psi_0+\psi_4)\right.$$

$$-v\left\{\left[(T+\mu)t-\frac{t^2}{2}\right] + \left[(T+\mu)^2 + \frac{(\xi\omega(T+\mu)+1)^2}{\Omega^2}\right]^{1/2}\frac{e^{-\xi\omega t}}{\omega}\sin(\Omega t+\psi_1+\psi_4)\right.$$

$$+\frac{(a^2+b^2)^{1/2}}{\omega}e^{-\xi\omega(T+\mu+t)}\cos(\Omega t+\psi_3+\psi_4) + \frac{e^{-\xi\omega(T+\mu+t)}}{4\omega^2(1-\xi^2)^{1/2}}$$

$$\times\sin[\Omega(T+\mu-t)+\psi_0-\psi_4] - \frac{e^{-\xi\omega(T+\mu-t)}}{4\omega^2(1-\xi^2)^{1/2}}\sin[\Omega(T+\mu-t)+\psi_0+\psi_4]$$

$$\left.+\frac{\Omega e^{-\xi\omega(T+\mu-t)}}{4\xi\omega^3(1-\xi^2)^{1/2}}\cos[\Omega(T+\mu-t)+\psi_0+\psi_4] - \left[(T+\mu)t_0-\frac{t_0^2}{2}\right]\right.$$

$$+C_1(T+\mu,t_0,\xi,\omega)\bigg\} \qquad (27)$$

$$x_1(t) = x_{10} + x_{20}(t-t_0) + \frac{x_{30}}{\omega(1-\xi^2)}\left[e^{-\xi\omega t_0}(t-t_0)\cos(\Omega t_0+\psi_0+\psi_4)\right.$$

$$\left.-\frac{e^{-\xi\omega t_0}}{\omega}\cos(\Omega t_0+\psi_0+2\psi_4) + \frac{e^{-\xi\omega t}}{\omega}\cos(\Omega t+\psi_0+2\psi_4)\right]$$

$$-v\left\{\left[(T+\mu)\frac{t^2}{2}-\frac{t^3}{6}\right] - \left[(T+\mu)^2 + \frac{(\xi\omega(T+\mu)+1)^2}{\Omega^2}\right]^{1/2}\frac{e^{-\xi\omega t}}{\omega^2}\sin(\Omega t+\psi_1+2\psi_4)\right.$$

$$-\frac{(a^2+b^2)^{1/2}}{\omega^2}e^{-\xi\omega(T+\mu+t)}\cos(\Omega t+\psi_3+\psi_4) + \frac{e^{-\xi\omega(T+\mu+t)}}{4\omega^3(1-\xi^2)^{1/2}}$$

$$\times\sin[\Omega(T+\mu-t)+\psi_0-2\psi_4] - \frac{e^{-\xi\omega(T+\mu-t)}}{4\omega^3(1-\xi^2)^{1/2}}\sin[\Omega(T+\mu-t)+\psi_0+2\psi_4]$$

$$+\frac{\Omega e^{-\xi\omega(T+\mu-t)}}{4\xi\omega^4(1-\xi^2)^{1/2}}\cos[\Omega(T+\mu-t)+\psi_0+2\psi_4] - \left[(T+\mu)t_0-\frac{t_0^2}{2}\right]t$$

$$+C_1(T+\mu,t_0,\xi,\omega)t + \frac{(T+\mu)t_0^2}{2} - \frac{t_0^3}{3} + C_0(T+\mu,t_0,\xi,\omega)\bigg\} \qquad (28)$$

From formula (28), letting t=T we can obtain

$$x_1(T) = x_1^0(T) - v\left\{\frac{(T-t_0)^3}{3} + \frac{\mu(T-t_0)^2}{2} + \Delta x_1(T,\mu,\xi,\omega)\right\} \qquad (29)$$

31

In the formula

$$x_1^0(T) = x_{10} + x_{20}(T - t_0) + \frac{x_{30}}{\omega(1 - \xi^2)} \Big[e^{-i\omega t_0}(T - t_0)\cos(\Omega t_0 + \psi_0 + \psi_4)$$

$$- \frac{e^{-i\omega t_0}}{\omega}\cos(\Omega t_0 + \psi_0 + 2\psi_4) + \frac{e^{-i\omega T}}{\omega}\cos(\Omega T + \psi_0 + 2\psi_4)\Big]$$

$$\Delta X_1(T, \mu, \xi, \omega) = -\Big[(T + \mu)^2 + \frac{(\xi\omega(T + \mu) + 1)^2}{\Omega^2}\Big]^{1/2} \frac{e^{-i\omega T}}{\omega^2}\sin(\Omega T + \psi_1 + 2\psi_4)$$

$$- \frac{(a^2 + b^2)^{1/2}}{\omega^2} e^{-i\omega(2T + \mu)}\cos(\Omega T + \psi_3 + \psi_4) + \frac{e^{-i\omega(2T + \mu)}}{4\omega^3(1 - \xi^2)^{1/2}}$$

$$\times \sin(\Omega\mu + \psi_0 - 2\psi_4) - \frac{e^{-i\omega\mu}}{4\omega^3(1 - \xi^2)^{1/2}}\sin(\Omega\mu + \psi_0 + 2\psi_4)$$

$$+ \frac{\Omega e^{-i\omega\mu}}{4\xi\omega^4(1 - \xi^2)^{1/2}}\cos(\Omega\mu + \psi_0 + 2\psi_4) + C_1(T + \mu, t_0, \xi, \omega)T$$

$$+ C_0(T + \mu, t_0, \xi, \omega)$$

From formula (27), letting t=T, we can obtain

$$x_2(T) = x_2^0(T) - v\Big\{\frac{(T - t_0)^2}{2} + \mu(T - t_0) + \Delta X_2(T, \mu, \xi, \omega)\Big\} \qquad (30)$$

In the formula

$$x_2^0(T) = x_{20} + \frac{x_{30}}{\omega(1 - \xi^2)}\big(e^{-i\omega t_0}\cos(\Omega t_0 + \psi_0 + \psi_4) - e^{-i\omega T}\cos(\Omega T + \psi_0 - \psi_4)\big)$$

$$\Delta X_2(T, \mu, \xi, \omega) = \Big[(T + \mu)^2 + \frac{(\xi\omega(T + \mu) + 1)^2}{\Omega^2}\Big]^{1/2} \frac{e^{-i\omega T}}{\omega}\sin(\Omega T + \psi_1 + \psi_4)$$

$$+ \frac{(a^2 + b^2)^{1/2}}{\omega} e^{-i\omega(2T + \mu)}\cos(\Omega T + \psi_3 + \psi_4) + \frac{e^{-i\omega(2T + \mu)}}{4\omega^2(1 - \xi^2)^{1/2}}$$

$$\times \sin[\Omega\mu + \psi_0 - \psi_4] - \frac{e^{-i\omega\mu}}{4\omega^2(1 - \xi^2)^{1/2}}\sin(\Omega\mu + \psi_0 + \psi_4)$$

$$+ \frac{\Omega e^{-i\omega\mu}}{4\xi\omega^3(1 - \xi^2)^{1/2}}\cos(\Omega\mu + \psi_0 + \psi_4) + C_1(T + \mu, t_0, \xi, \omega)$$

Because the system should reach the target group when t=T, it should satisfy

$$x_1(T) + \mu\, x_2(T) = 0$$

From Formulas (29) and (30), we can obtain

32

$$x_1^0(T) + \mu x_2^0(T) - v \left\{ \frac{(T-t_0)^3}{3} + \mu (T-t_0) + \mu^2 (T-t_0) + \Delta X_1(T, \mu, \xi, \omega) \right.$$

$$\left. + \mu \Delta X_2(T, \mu, \xi, \omega) \right\} = 0$$

We can find v from this formula.

$$v = \frac{x_1^0(T) + \mu x_2^0(T)}{\frac{(T-t_0)^3}{3} + \mu (T-t_0)^2 + \mu^2 (T-t_0) + \Delta X_1(T, \mu, \xi, \omega) + \mu \Delta X_2(T, \mu, \xi, \omega)}$$

$$(31)$$

When we substitute formula (31) into formula (__), obtain the optimal control law:

$$\bar{u}(t) = -[x_1^0(T) + \mu x_2^0(T)] \cdot \left\{ (T + \mu - t) - \frac{2\xi}{\omega} + \frac{1}{\omega} e^{-\xi \omega (T + \mu - t)} \right.$$

$$\times \left[2\xi \cos \Omega (T + \mu - t) + \frac{2\xi^2 - 1}{(1 - \xi^2)^{1/2}} \sin \Omega (T + \mu - t) \right] \right\} \cdot \left\{ \frac{(T-t_0)^3}{3} \right.$$

$$\left. + \mu (T-t_0)^2 + \mu^2 (T-t_0) + \Delta X_1(T, \mu, \xi, \omega) + \mu \Delta X_2(T, \mu, \xi, \omega) \right\}^{-1}$$

$$(32)$$

When $t=t_0$, the optical guidance law is

$$\bar{u}(t_0) = -[x_1^0(T) + \mu x_2^0(T)] \left\{ (T + \mu - t_0) - \frac{2\xi}{\omega} + \frac{1}{\omega (1 - \xi^2)^{1/2}} e^{-\xi \omega (T + \mu - t_0)} \right.$$

$$\times \sin [\Omega (T + \mu - t_0) + \phi_0] \right\} \left\{ \frac{(T-t_0)^3}{3} + \mu (T-t_0)^2 + \mu^2 (T-t_0) \right.$$

$$\left. + \Delta X_1(T, \mu, \xi, \omega) + \mu \Delta X_2(T, \mu, \xi, \omega) \right\}^{-1}$$

$$(33)$$

The above formula can be rewritten as

$$\bar{u}(t_0) = -K_L(T, \mu, \xi, \omega)[x_{10} + x_{20}(T + \mu$$

$$- t_0)] - L_L(T, \mu, \xi, \omega) x_{30}$$

$$(34)$$

In the formula

33

$$K_L(T, \mu, \xi, \omega) = \Big\{ (T + \mu - t_0) - \frac{2\xi}{\omega} + \frac{1}{\omega(1 - \xi^2)} e^{-\xi\omega(T+\mu-t_0)}$$

$$\times \sin[\Omega(T + \mu - t_0) + \psi_0] \Big\} \Big\{ \frac{(T - t_0)^3}{3} + \mu(T - t_0)^2 + \mu^2(T - t_0)$$

$$+ \Delta X_1(T, \mu, \xi, \omega) + \mu \Delta X_2(T, \mu, \xi, \omega) \Big\}^{-1}$$

$$L_L(T, \mu, \xi, \omega) = \frac{1}{\omega(1 - \xi^2)} \Big[e^{-\xi\omega t_0}(T + \mu - t_0)\cos(\Omega t_0 + \psi_0 + \psi_4)$$

$$- \frac{1}{\omega} e^{-\xi\omega t_0}\cos(\Omega t_0 + \psi_0 + 2\psi_4) + \frac{1}{\omega} e^{-\xi\omega T}\cos(\Omega T + \psi_0 + 2\psi_4)$$

$$- \mu e^{-\xi\omega T}\cos(\Omega T + \psi_0 + \psi_4) \Big\} \Big\{ \frac{(T - t_0)^3}{3} + \mu(T - t_0)^2 + \mu^2(T - t_0)$$

$$+ \Delta X_1(T, \mu, \xi, \omega) + \mu \Delta X_2(T, \mu, \xi, \omega) \Big\}^{-1}$$

The γ_1, γ_3, a, b and the t_f in this section should all be replaced by $T + \mu$.

In optimal control law formula (33) or (34), the μ is still undetermined. Only when the μ is determined can we calculate and completely determine the optimal control law. For this reason, we used the condition of $x_3(T)=0$. Although this condition has already been considered in the limit value conditions, yet because it is established in the optimal control process, this optimal control law is unrelated to λ_3 and therefore the condition of $x_3(T)=0$ is still not really used. In order to guarantee not separating from this curved surface again after introducing the system into the zero control intercept curved surface, we must select the μ in this way so that $x_3(T)=0$. From formula (26), letting t=T, we can obtain:

34

$$x_3(T) = -v \left\{ \mu - \left[(T-\mu)^2 - \frac{(\xi\omega(T-\mu)-1)^2}{\Omega^2} \right]^{1/2} e^{-\xi\omega T}\sin(\Omega T - \psi_1) \right.$$

$$- \frac{e^{-\xi\omega(2T+\mu)}}{4\omega(1-\xi^2)^{1/2}}\sin(\Omega\mu+\psi_0) - (a^2+b^2)^{1/2}e^{-\xi\omega(2T+\mu)}$$

$$\times \cos(\Omega T + \psi_3) - \frac{e^{-\xi\omega\mu}}{4\omega(1-\xi^2)^{1/2}}\sin(\Omega\mu+\psi_0) + \frac{\Omega e^{-\xi\omega\mu}}{4\xi\omega^2(1-\xi^2)^{1/2}}$$

$$\left. \times \cos(\Omega\mu-\psi_3) \right\} + \frac{x_{30}}{1-\xi^2}e^{-\xi\omega T}\cos(\Omega T + \psi_2) = 0$$

By substituting in formula (31), we can obtain

$$-[x_1^0(T)+\mu x_2^0(T)] \left\{ \mu - \left[(T-\mu)^2 + \frac{(\xi\omega(T+\mu)-1)^2}{\Omega^2} \right]^{1/2} e^{-\xi\omega T}\sin(\Omega T + \psi_1) \right.$$

$$- \frac{e^{-\xi\omega(2T+\mu)}}{4\omega(1-\xi^2)^{1/2}}\sin(\Omega\mu+\psi_0) - (a^2+b^2)^{1/2}e^{-\xi\omega(2T+\mu)}\cos(\Omega T + \psi_3)$$

$$\left. - \frac{e^{-\xi\omega\mu}}{4\omega(1-\xi^2)^{1/2}}\sin(\Omega\mu+\psi_0) + \frac{\Omega e^{-\xi\omega\mu}}{4\xi\omega^2(1-\xi^2)^{1/2}}\cos(\Omega\mu+\psi_0) \right\}$$

$$\times \left\{ \frac{(T-t_0)^3}{3} + \mu(T-t_0)^2 + \mu^2(T-t_0) + \Delta X_1(T,\mu,\xi,\omega) \right.$$

$$\left. + \mu\Delta X_2(T,\mu,\xi,\omega) \right\}^{-1} + \frac{x_{30}}{1-\xi^2}e^{-\xi\omega T}\cos(\Omega T + \psi_2) = 0 \qquad (35)$$

This is a high order transcendental equation which can use a
numerical solution to solve μ. There are possibly many μ
values to satisfy equation (35). At this time, we should take
the smallest one among the μ which is larger than zero.
Naturally, it is also possible that no μ exists which can
satisfy equation (35). Under these conditions, the system is
guided to the zero control intercept curved surface, yet it
cannot cause the system to be maintained in this curved surface.
At this time, it loses significance for the guidance of the zero
control intercept curved surface. However, physically, control
to cause the relative acceleration be zero exists and therefore
the equation should have a solution.

When $\omega \to \infty$, the characteristic loss of the missile's
second order link becomes particles with instantaneous response.
At this time, $K_L(T, \mu, \xi, \omega)$ and $L_L(T, \mu, \xi, \omega)$ of formula (34)
become

$$K_L(T, \mu, \xi, \omega) = \frac{T + \mu - t_0}{\dfrac{(T - t_0)^3}{3} + \mu(T - t_0)^2 + \mu^2(T - t_0)}$$

$$L_L(T, \mu, \xi, \omega) = 0$$

Optimal guidance law $\bar{u}(t_o)$ changes to

$$\bar{u}(t_0) = -\frac{x_{10} + x_{20}(T + \mu - t_0)}{\dfrac{(T - t_0)^2}{3} + \mu(T - t_0)^2 + \mu^2(T - t_0)}(T + \mu - t_0) \qquad (36)$$

This is the result obtained by guiding the instantaneous response particles toward zero control intercept curved surface L [3].

IV.   Concluding Remarks

Above, we obtained the optimal guidance laws of formulas (20) and (34) for missiles with second order characteristics for two types of target groups. These two formulas are similar in form. If the missile's acceleration is expressed by the rate of change of the line of sight rotation angular velocity and angular velocity, and we let

$$T - t_0 = -\frac{x_{10}^T(\alpha x_{10} + \beta x_{20})}{x_{20}^T(\alpha x_{10} + \beta x_{20})}$$

$$T + \mu - t_0 = -\frac{x_{10}^T(\alpha x_{10} + \beta x_{20})}{x_{20}^T(\alpha x_{10} + \beta x_{20})}$$

then formulas (20) and (34) can be expressed as [1]:

$$\bar{u}(x_{10},\ x_{20},\ \bar{\omega}_0, \dot{\bar{\omega}}_0,\ \alpha,\ \beta,\ \xi,\ \omega,\ \mu)$$

$$= -L_L(x_{10},\ x_{20},\ \alpha,\ \beta,\ \xi,\ \omega,\ \mu)\frac{x_{10}^2}{x_{12}^T(\alpha x_{10}+\beta x_{20})}$$

$$\times \left[\frac{x_{30}^T(\alpha x_{10}+\beta x_{20})}{x_{10}^2}\,x_{10}+\dot{\bar{\omega}}_0\times(\alpha x_{10}+\beta x_{20})\right]+\left[K_L(x_{10},x_{20},\ \alpha,\ \beta,\ \xi\ \omega,\ \mu)\right.$$

$$\times \frac{x_{10}^2}{x_{20}^T(\alpha x_{10}+\beta x_{20})}-2L_L(x_{10},\ x_{20},\ \alpha,\ \beta,\ \xi,\ \omega,\ \mu)$$

$$\left.\times \frac{x_{10}^T x_{20}}{x_{12}^T(\alpha x_{10}+\beta x_{20})}\right]\bar{\omega}_0\times(\alpha x_{10}+\beta x_{20}) \tag{37}$$

In the formula, $\overline{\omega}$ and $\dot{\omega}$ are separately the angular velocity of the line of sight and the angular acceleration; a and β are real numbers and can be selected according to requirements.

It can be seen from formula (37) that the optimal guidance law for missiles with second order characteristics is composed of proportional guidance with a variable coefficient and a correction item related to the acceleration and line of sight angular acceleration under specified transit time conditions. Naturally, to realize this type of guidance law, aside from needing to measure the angular velocity of the line of sight, it is also necessary to measure the rate of change and acceleration of the line of sight angular velocity. Although the computation of its coefficient is relatively complex, yet they are already known functions of x_{10}, x_{20}, a, β, ξ, ω and μ. We believe they are not difficult to complete in today's flourishing of electronic technology. Because the mathematical models selected for the missiles went a step further than the mathematical models provided by the listed references, we will thus have even higher guidance precision.

References

[1] Wang Chaozhu, Optimal Intercept Guidance Laws, Journal of Aeronautics, No. 4, 1979.

[2] Systems Institute of the Chinese Academy of Sciences, Extreme Value Control and the Principle of the Maximum, Science Press, 1980.11.

References (continued)

[3] Han Jingqing et al, The Guidance Laws in the Problem of
     Interception, Defense Industries Press, 1977.6

[4] R. G. Cottrell, "Optimal intercept guidance for short-Range
     tactical Missiles" AIAA J9:7 (1971).

[5] Garber, V., "Optimum intercept laws of acceleratary target"
     AIAA J Vol 6, No. 11 (19 68).

38